Influence of Hydrogen on the Mechanism of Permanent Passivation of Boron–Oxygen Defects in p-Type Czochralski Silicon

Nitin Nampalli, Brett J. Hallam, Catherine E. Chan, Malcolm D. Abbott, and Stuart R. Wenham

***Abstract*—Strong evidence is provided for the critical role of hydrogen in the permanent passivation of boron–oxygen (B–O) defects in p-type Czochralski silicon. In particular, the impact of rapid thermal processing (firing), plasma exposure, and hydrogen-containing dielectrics on B–O defect passivation is explored. Importantly, no permanent passivation of B–O defects is observed in samples fired bare (both with and without exposure to a hydrogen-rich plasma prior to firing) and in nonfired samples coated with hydrogenated silicon nitride (SiN_x:H). In contrast, samples with SiN_x:H layers present during firing resulted in significant levels of B–O passivation, even at firing temperatures as low as ∼500 °C. Increasing peak firing temperatures (T_{peak}) appeared to correlate to increased B–O passivation ability; however, increasing T_{peak} above a value of 670 °C resulted in suboptimal levels of surface and bulk passivation. These observations are explained within a hydrogen-based model for permanent passivation of B–O defects. Implications for nonhydrogen-based models are also discussed.**

***Index Terms*—Boron-oxygen defect, hydrogen passivation, light-induced degradation, rapid thermal processing, regeneration.**

I. Introduction

OXYGEN-RICH boron-doped Czochralski (Cz) silicon is known to undergo degradation in minority carrier lifetime during carrier injection due to the formation of recombination-active boron–oxygen (B–O) defects in the wafer bulk. This reduces the efficiency of solar cells made using such substrates. In addition to temporary (but unstable) deactivation of the B–O defect by dark annealing, it is possible to permanently deactivate the B–O defect through an illuminated annealing process, in which the B–O defect is effectively in a recombination inactive "regenerated" state [1]. The relationship between these three states has been described by Herguth *et al.* in an empirical three-state model [2] that has since been expanded upon [3].

Of particular interest is the permanent passivation of B–O defects and the conditions required to quickly and effectively passivate the defect. Achieving this state appears to require three process steps: Wafers or cells must 1) be coated with hydrogen-containing dielectric layers [4], [5]; 2) undergo a high-temperature anneal (generally a rapid thermal anneal at temperatures above 600 °C) [6], [7]; and 3) undergo a subsequent illuminated annealing process.

The kinetics of the illuminated annealing process and its impact on B–O defect passivation are mostly well known [3], and annealing optimization is an area of active research by many groups [8], [9]. The important roles of the firing process and the dielectric layers have, likewise, long been known [4]; however, the reasons for their importance continue to be debated in the literature [7], [10], [11], as multiple mechanisms for defect passivation have been proposed. Of these, passivation by hydrogen [9], [12] and passivation by boron nanoprecipitates (BNPs) [7], [13], [14] are the two primary hypotheses. Further, the role of plasma exposure has also been suggested as being somehow critical to the passivation process as plasma exposure is ubiquitous in cases where B–O passivation has been demonstrated [10].

In prior work, it was demonstrated that any persistent species introduced solely by plasma processing are unlikely to cause B–O defect passivation [15]. Second, no evidence of permanent lifetime recovery was revealed in bare-fired wafers, suggesting that B–O defect passivation is not a purely thermal process [16]. The influence of peak firing temperature on B–O defect passivation was also explored in our most recent work [17]. In this study, statistically significant levels of B–O defect passivation are demonstrated at firing temperatures as low as 500 °C. New analysis of prior work is also presented to 1) further clarify the impact of dielectric layers and firing conditions on B–O defect passivation, and 2) provide new insights into the passivation mechanism.

II. General Experimental Setup

A. Sample Preparation

Symmetrical test structures were prepared from commercial-grade boron-doped Cz wafers (1.6 Ω·cm), which were alkaline textured followed by acidic neutralization and RCA cleaning. A double-sided gettering diffusion was then performed using a $POCl_3$ tube furnace. The resulting emitter (70 Ω/sq) was then etched to minimize the impact of the gettered impurities on minority carrier lifetime measurements. The wafers were subsequently RCA cleaned, and a second $POCl_3$ diffusion was performed to obtain a lightly diffused emitter (∼200 Ω/sq) to aid in surface passivation (see [15] for diffusion recipe details).

Following phosphosilicate glass removal, wafers were either coated with hydrogenated silicon nitride (SiN_x:H) deposited

Manuscript received June 1, 2015; revised July 23, 2015; accepted August 4, 2015. Date of publication August 28, 2015; date of current version October 19, 2015. This work was supported by the Australian Renewable Energy Agency under Grant ARENA-1-060 and by the U.K. Institution of Engineering and Technology through the A. F. Harvey Engineering Prize. Responsibility for the views, information, or advice expressed herein is not accepted by the Australian Government.

The authors are with the School of Photovoltaic and Renewable Energy Engineering, University of New South Wales, Sydney, N.S.W. 2052, Australia (e-mail: n.nampalli@student.unsw.edu.au; brett.hallam@unsw.edu.au; catherine.chan@unsw.edu.au; m.abbott@unsw.edu.au; s.wenham@unsw.edu.au).

Color versions of one or more of the figures in this paper are available online at http://ieeexplore.ieee.org.

Digital Object Identifier 10.1109/JPHOTOV.2015.2466457

on both surfaces using direct plasma-enhanced chemical vapor deposition (PECVD) (SiN_x:H Deposition 1) or left uncoated (bare). Certain groups of wafers were subsequently fired in a SierraTherm infrared fast-firing belt furnace, while other groups were not fired. Thermal history of the firing processes was measured using a Datapaq Q18 thermal profiler on dummy wafers prepared identically to the samples.

B. Defect Manipulation

At this stage, the samples varied in their treatments regarding two of the three process steps required for B–O passivation: 1) presence/absence of a hydrogen-rich dielectric (SiN_x:H) and 2) firing conditions. In order to minimize the differences in surface recombination between the various samples and to study the bulk properties of the B–O defect, the following four process steps were performed on all samples: 1) Any SiN_x:H layers present postfiring were stripped and new SiN_x:H layers deposited on all samples (SiN_x:H Deposition 2); 2) wafers were then made to undergo a light-induced degradation step (LID-1) until completely degraded; 3) an illuminated annealing step was performed to induce B–O defect passivation; and 4) wafers were again irradiated (LID-2) to ensure the stability of B–O passivation.

All LID steps were performed for 48 h at 40 °C under a light intensity of ∼0.8 suns. Illuminated annealing was done for 2 h on a hot plate at 172 °C under a light intensity of ∼0.65 suns. Note that halogen lights were used as illumination sources for both processes, with irradiance measured using a silicon reference cell. SiN_x:H layers were deposited at 350 °C on both sides of the wafers using an MAiA PECVD system. The resulting SiN_x:H layers were 80 nm thick, with a refractive index of 2.08 at 633 nm. Identical SiN_x:H layers were deposited before and after firing. Further sample preparation details can be found in [15].

C. Characterization and Analysis

Characterization was performed by measuring effective minority carrier lifetime ($\tau_{\rm eff}$) using the Sinton WCT-120 quasi-steady-state photoconductance tester. Following Auger-correction using the Richter model [18], lifetime is extracted under low injection conditions at an excess minority carrier concentration (Δn) of 2×10^{14} cm^{-3}, which is equivalent to $0.02 \times N_{\rm A}$ ($N_{\rm A}$ being the base acceptor doping concentration).

Typically, $\tau_{\rm eff}$ measured on as-fired samples is directly used as a metric for measuring B–O defect-related Shockley–Read–Hall recombination and for calculating normalized defect concentrations. However, this method relies on the assumptions that 1) $\tau_{\rm eff}$ is not limited by surface recombination and that 2) changes in surface recombination are not significant between processing steps. However, it has been shown that a combination of high-temperature firing and extended lower temperature annealing in the time and temperature regimes similar to those in this work can cause degradation of surface passivation [9]. Hence, to more accurately track changes in bulk properties, we first used bulk minority carrier lifetime ($\tau_{\rm bulk}$) as the metric for bulk characterization. Second, as previously mentioned, the SiN_x:H layers, if present on the wafers, are redeposited after firing to achieve uniform surface passivation in all samples. The methods used to extract $\tau_{\rm bulk}$, $\tau_{\rm eff}$, and emitter dark saturation current density ($J_{0\rm E}$) are detailed elsewhere [15].

III. Role of Hydrogen Source in Defect Passivation

Hydrogen has long been suspected as the species responsible for B–O "regeneration" (permanent passivation) [11], [12]. This is based on hydrogen's well-known ability to bind to and passivate various defects in silicon, as well as its ubiquitous presence in passivating dielectrics such as PECVD SiN_x:H. Moreover, permanent B–O defect passivation has so far not been demonstrated in wafers with dielectrics in which hydrogen is absent [4].

However, alternative explanations for permanent passivation have also been proposed. Plasma exposure as a prerequisite for B–O defect passivation was initially proposed by Lim *et al.* [10] on the basis of 1) the fact that plasma exposure is known to occur during most dielectric deposition methods, including direct-plasma PECVD and plasma-assisted atomic layer deposition, and 2) the absence of B–O defect passivation with SiN_x films without plasma exposure, such as remote-plasma PECVD [10] or low-pressure CVD-deposited films [4]. Further, plasma exposure is known to greatly improve the rate and magnitude of B–O defect passivation in both dielectric-coated [10] and bare wafers [11]. Hence, a plasma-introduced species may be assumed to cause permanent passivation.

The other alternative hypothesis based on the capture of B–O defect precursors by BNPs, which are theorized to form under favorable thermal conditions during firing, was presented by Voronkov *et al.* [13] to explain the observed kinetics of the illuminated annealing process. A theoretical treatment of the relation between BNP formation and cooling rate during firing was provided in more recent work [14], and experimental work supporting the hypothesis was presented by Walter *et al.*, who suggested that the cooling rate between 575 °C and 625 °C is critical for BNP formation [7]. In the latter work, hydrogen was also proposed to be noncritical to B–O passivation based on the observed modulation of annealing and degradation kinetics with changing firing conditions in wafers coated with hydrogen-lean Al_2O_3.

In order to distinguish between thermal effects, hydrogenation, and plasma exposure, controlled trials were performed in previous studies [15], [16]. We expand on the analysis of these results in this study.

A. Experimental Details

Following phosphosilicate glass removal as described previously in Section II-A, identically prepared wafers were divided into five groups that A) neither had dielectric layers nor were fired; B) were fired with no dielectric layers present during firing (i.e., fired bare); C) were fired bare but with prior plasma exposure through PECVD deposition of SiN_x:H layers, which were subsequently stripped [15]; D) had PECVD SiN_x:H layers deposited but were not fired; and E) were fired with SiN_x:H present during firing.

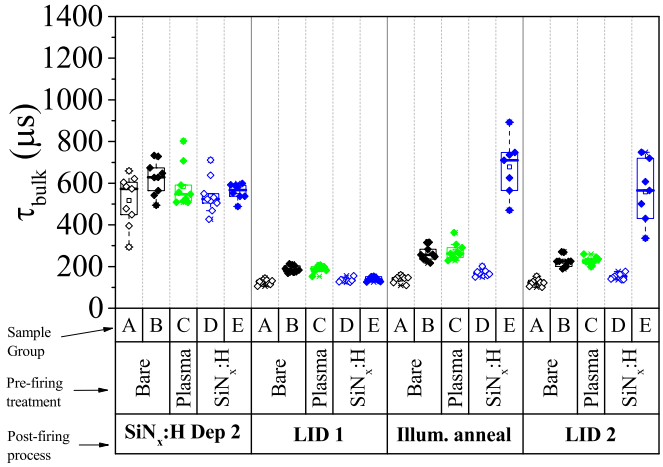

Fig. 1. Box-plot tracking the change in τ_{bulk} after each postfiring step for (A) a control wafer—nonfired, bare (black, hollow); (B) a fired bare wafer (black, filled); (C) a fired bare wafer with prior plasma exposure (green, filled); (D) a nonfired SiN_x:H-coated wafer (blue, hollow); and (E) a fired SiN_x:H-coated wafer (blue, filled). Only wafers fired with SiN_x:H present during firing undergo stable recovery of lifetime, indicating permanent passivation of B–O defects. Includes data from [15] and [16].

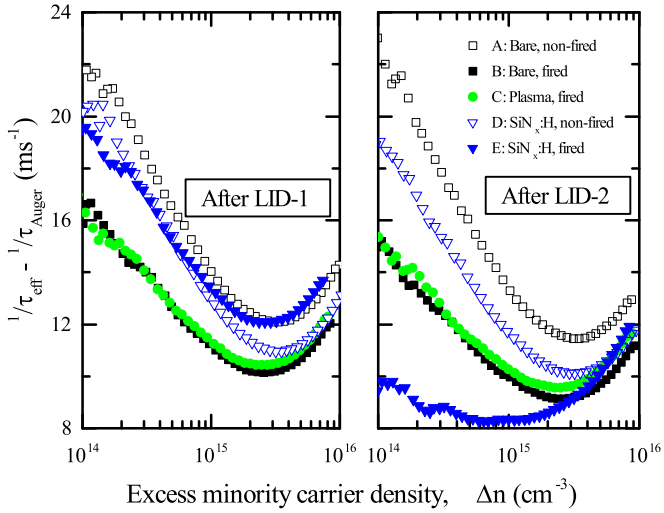

Fig. 2. Auger-corrected inverse effective lifetime as a function of excess minority carrier density measured after LID-1 (left) and after LID-2 (right) for the five wafer groups (A, B, C, D, and E) presented in Fig. 1. Only Group E, fired with SiN_x:H present (blue, filled), displays stable reduction in B–O defect related injection-dependence behavior in low injection ($\Delta n \leq 10^{15}$ cm^{-3}) following the illuminated annealing process.

New SiN_x:H layers were then deposited on all wafers after firing, with any existing SiN_x:H layers stripped prior to redeposition. Wafers were then subjected to the sequence of steps described previously in Section II-B, namely, light soaking (for degradation), illuminated annealing, and light soaking again (for stability testing).

B. Results

Fig. 1 shows the change in τ_{bulk} over the process sequence described earlier for groups A through E. It can be seen that illuminated annealing causes an increase in the observed τ_{bulk} for all fired samples (filled data points); however, the improvement in τ_{bulk} for the wafer with a hydrogen source (SiN_x:H) present during firing is significantly higher, and importantly, is stable even after 48 h of light soaking (LID-2). Analysis of the injection-dependent lifetime curves revealed that the B–O defect is in a permanently passivated state in Group E at the end of LID-2 [15]. In comparison, there was no permanent recovery in any of the other four groups.

Note that τ_{bulk} after initial degradation and after illuminated annealing appear to be slightly higher for plasma-exposed (green) and bare-fired wafers (black, solid). The cause for this was unrelated to the B–O defect and is demonstrated in Fig. 2, which compares injection-dependent inverse lifetime curves measured after LID-1 (lifetime prior to illuminated annealing) and LID-2 (stabilized lifetime after illuminated annealing).

Prior to illuminated annealing, all wafers displayed similar injection-dependent lifetime behavior under low injection ($\Delta n \leq 10^{15}$ cm^{-3}) typical of the B–O defect [15], indicating the presence of recombination-active B–O defects at this step. Only the SiN_x:H-fired sample (Group E) displayed a severe reduction of injection dependence after illuminated annealing and subsequent light soaking, while injection dependence persisted in Groups A through D. This confirms that the small

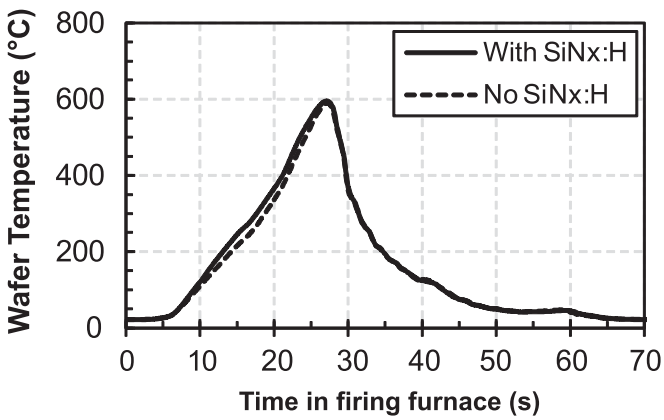

Fig. 3. Thermal profiles of rapid firing process measured on wafers with (solid line) and without (dotted line) SiN_x:H layers.

improvements in τ_{bulk} seen after illuminated annealing in groups A through D were not due to B–O defect passivation.

Since it may also be argued that the absence of SiN_x:H may affect the thermal properties of the wafers during firing, the temperature profiles of bare (Group B) and SiN_x:H-coated wafers (Group E) were measured during the firing process (see Fig. 3).

However, the firing profiles were found to be almost identical, with the only difference being that bare-fired wafers displayed a slightly lower temperature ramp up rate in the first few seconds of the firing process. Importantly, the peak firing temperature ($T_{\mathrm{peak}} = 600$ °C), cool-down profiles, and cooling rates were found to be equivalent for both samples.

C. Discussion

Our results have two main implications. First, the lack of passivation during illuminated annealing in the plasma-exposed

wafer suggests that plasma exposure is not the primary source of the species directly responsible for B–O defect passivation. This eliminates the role of plasma exposure as the cause of B–O defect passivation. However, this does not rule out the possibility that plasma exposure enhances the diffusion of species responsible for B–O passivation [19], [20].

This interpretation is consistent with a hydrogen-based B–O defect passivation mechanism wherein a hydrogen source (PECVD SiN_x:H in this case) releases hydrogen into the bulk during the firing process. In this model, plasma exposure enhances hydrogen diffusion during the deposition process, most likely through surface damage-assisted mechanisms [19] or by otherwise enhancing the formation of favorable bound hydrogen states [20] that later release hydrogen into the bulk during firing. This interpretation is also supported by other studies that show enhanced passivation in plasma-exposed wafers (but which are subsequently coated with hydrogen-containing dielectrics) [5]. The lack of a barrier to prevent the out-diffusion of any hydrogen introduced by the plasma exposure may also explain why bare plasma-exposed wafers do not undergo B–O passivation.

Second, it can be concluded that rapid firing and/or rapid cooling alone is insufficient to induce B–O defect passivation. This casts doubt over the mechanism of B–O passivation via BNPs [13], which are theorized to form during the rapid cooling stage of the firing step purely by thermal action [14] and without the assistance of hydrogen-based species [7]. While the presence, formation, and passivation-enhancing properties of BNPs cannot themselves be ruled out, the fact that hydrogen appears to play a critical role in B–O defect passivation suggests either that hydrogen plays a more important role in BNP formation than previously assumed [14] or that BNPs do not greatly influence B–O defect passivation.

IV. Influence of Firing Conditions

Although the critical role of hydrogen in B–O passivation has been made clear, the mechanism of B–O passivation remains difficult to confirm due to the strong influence of firing conditions on passivation rates. Recent studies have shown that B–O defect passivation is highly influenced by high-temperature steps performed prior to the illuminated annealing process.

In particular, peak sample temperature during firing (T_{peak}) [6], [7], hold time at peak width (or thermal budget) [6], cooling rates in different temperature regimes [7], [9], and firing speed are known to directly influence not only the maximum achievable passivation level for a particular dielectric, but the kinetics of the permanent passivation process as well. Further, this behavior has been attributed to both hydrogen [6] and BNPs [7].

In the BNP model, T_{peak} and cooling rates are directly linked to the formation of BNPs, with the cooling rate between 575 °C and 625 °C proposed as being critical parameter for the precipitation of BNPs [7], [14]. Subsequent annealing steps are theorized to change the size and number of precipitates, thereby changing the passivation efficacy of BNPs.

T_{peak} and cooling rates are also proposed to be important in the hydrogen model. Here, cooling quickly is thought to result in hydrogen being in a favorable bound state within the bulk [9], with higher T_{peak} and shorter process times thought to result in better net retention of hydrogen in the bulk. Net retention is, in turn, a function of hydrogen effusion loss from the bulk and in-diffusion of hydrogen from the hydrogen source, both of which are temperature-dependent processes.

In order to distinguish between the two mechanisms, we attempt to find a lower limit to the temperature required for B–O passivation.

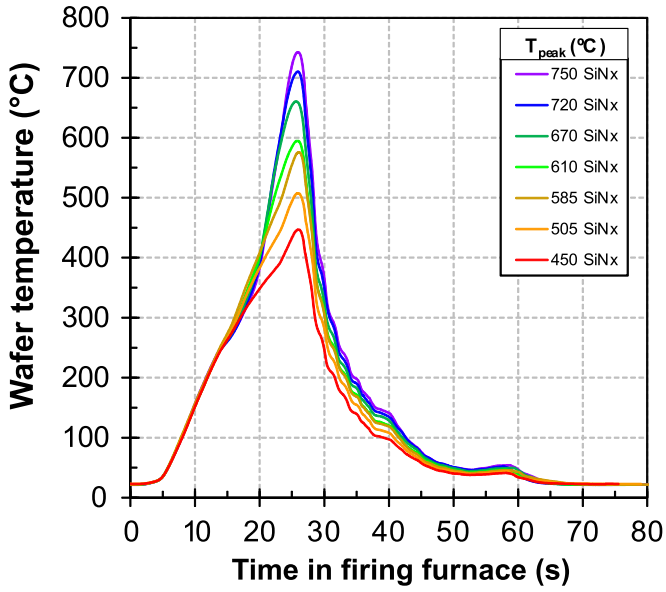

Fig. 4. Exemplary thermal profiles for various furnace recipes used in this study, denoted in the legend by the process T_{peak}.

A. Experimental Details

A group of SiN_x:H-coated samples (corresponding to wafer group E) were separately fired by varying the set point for T_{peak} between 550 °C and 850 °C while maintaining the belt speed at 8.5 cm/s. The resulting thermal profiles were measured on dummy wafers to determine the ramp-up rates, cool-down rates, and thermal budget of each firing treatment. As before, SiN_x:H layers were stripped and redeposited after firing, after which, the wafers underwent the same series of steps as earlier to manipulate the state of the B–O defect (as described in Section II-B).

B. Results

Fig. 4 shows the thermal profiles achieved for the various firing recipes used.

T_{peak} values between 450 °C and 750 °C were achieved, with very similar thermal history, thermal budget (defined as the area under the curve), and almost identical cooling rates below 350 °C. Hence, differences between profiles were primarily in the T_{peak} and thermal ramp-up/cooling rates above 350 °C. Cooling rates between 350 °C and T_{peak} were found to vary from 30 °C/s ($T_{\mathrm{peak}} = 450$ °C) to 115 °C/s ($T_{\mathrm{peak}} = 750$ °C).

The effect of the firing treatments on measured τ_{bulk} is as shown in Fig. 5, which plots the evolution of τ_{bulk} after firing,

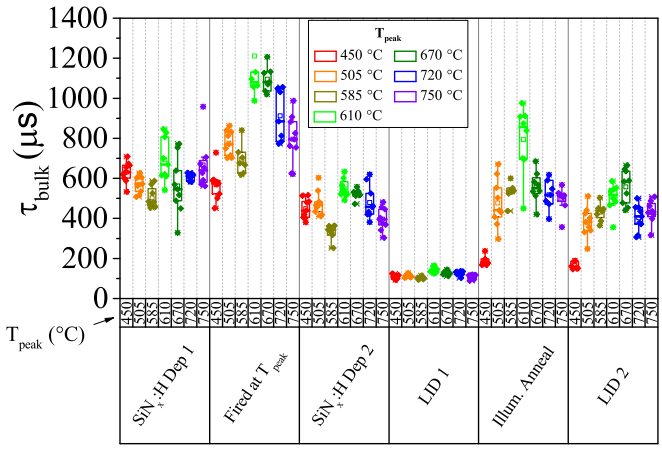

Fig. 5. Box-plot tracking the change in $\tau_{\rm bulk}$ with the sample process sequence after the initial SiN_x:H deposition step for wafers fired at various peak temperatures ($T_{\rm peak}$). Increasing $T_{\rm peak}$ does not necessarily result in better B–O defect passivation after illuminated annealing; instead, an optimum $T_{\rm peak}$ exists at 670 °C.

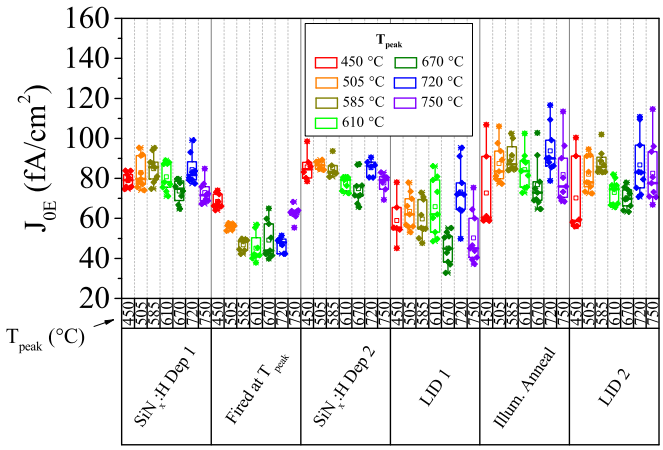

Fig. 6. Box-plot tracking the change in $J_{0\rm E}$ with the sample process sequence after the initial SiN_x:H deposition step for wafers fired at various $T_{\rm peak}$ settings. $J_{0\rm E}$ immediately after firing displays maximum reduction at $T_{\rm peak} = 670$ °C, the same temperature at which B–O passivation efficacy is maximum.

SiN_x:H redeposition, complete degradation, illuminated annealing, and a final LID process for stability testing.

It can be seen in Fig. 5 that in spite of similar initial values of $\tau_{\rm bulk}$ after LID-1, the net gain in $\tau_{\rm bulk}$ due to B–O defect passivation at the end of LID-2 is highly dependent on $T_{\rm peak}$. More importantly, B–O defect passivation efficacy increased with $T_{\rm peak}$ until $T_{\rm peak} = 670$ °C and then decreased for higher firing temperatures. Interestingly, permanent improvement in $\tau_{\rm bulk}$ was significant even for the wafer fired at the lowest $T_{\rm peak}$ value (450 °C) and was significantly higher for a marginally higher $T_{\rm peak}$ of 505 °C. Analysis of the $J_{0\rm E}$ extracted for these wafers (see Fig. 6) revealed that $J_{0\rm E}$ immediately after firing responded to a changing $T_{\rm peak}$ in a similar way to the change in $\tau_{\rm bulk}$. Prior to firing, all groups were observed to have a similar $J_{0\rm E}$ value of $\sim$80 fA/cm^2. However, immediately after firing, $J_{0\rm E}$ appeared to decrease with increasing $T_{\rm peak}$ until a minimum of $\sim$40 fA/cm^2 was reached for $T_{\rm peak} = 670$ °C.

Increasing $T_{\rm peak}$ beyond this temperature caused $J_{0\rm E}$ to increase once again, suggesting a deterioration in surface passivation beyond $T_{\rm peak} = 670$ °C. Subsequent redeposition of SiN_x:H caused a "reset" in $J_{0\rm E}$ values back to $\sim$80 fA/cm^2, albeit with a larger spread in data points. $J_{0\rm E}$ continued to retain a weak dependence on $T_{\rm peak}$ after LID–1, although the spread in the data made it difficult to confirm such a dependence. Nonetheless, it was clear that suboptimal firing temperatures simultaneously reduced the quality of surface passivation and reduced B–O passivation efficacy, suggesting a correlation between the two phenomena.

C. Discussion

The evidence of permanent B–O passivation at firing temperatures less than 505 °C provides important insights into the mechanism for B–O passivation. BNPs were hypothesized to form during the rapid cooling phase of the firing process in the temperature range between 575 and 625 °C [7], [14]—well above the temperature range in which B–O passivation has been observed in this study. Hence, it can be concluded that BNP formation either 1) occurs at temperatures lower than those suggested earlier, or 2) does, in fact, occur in the proposed temperature regimes, but does not impact B–O passivation, or 3) does not occur.

However, our observations are consistent with the hydrogenation-based model for B–O defect passivation as improvements in $\tau_{\rm eff}$ in SiN_x:H coated wafers at $T_{\rm peak}$ values as low as 400 °C have been reported by Bousbih *et al.*, who correlate lifetime improvements to Si-H bond dissociation within the SiN_x:H film [20].

This suggests a direct link between net hydrogen incorporation into the wafer bulk during firing and B–O passivation efficacy. Hence, the temperature profiles at higher firing temperatures ($T_{\rm peak} = 720$ °C, 750 °C) can be thought of as a regime in which out-effusion of hydrogen dominates over in-effusion as $T_{\rm peak}$ increases, resulting in lower hydrogen retention in the bulk compared with $T_{\rm peak} = 670$ °C. This lowers passivation efficacy even though the same illuminated annealing process is applied. Evidence of optimally minimum $J_{0\rm E}$ obtained at the same $T_{\rm peak}$ value adds further weight to this interpretation since increased hydrogen retention is expected to improve both surface passivation and B–O defect passivation. Additionally, increased $J_{0\rm E}$ values seen in wafers fired at suboptimally high $T_{\rm peak}$ values (720 °C, 750 °C) may also be due to surface or dielectric damage induced at such temperatures. However, the presence of such surface damage could not be confirmed.

Note that the $T_{\rm peak}$ observed for achieving optimum surface and bulk passivation may be specific to the SiN_x:H film used in this study as other studies have reported rates of B–O passivation to consistently increase with $T_{\rm peak}$ up to 850 °C without flattening or peaking [6]. Specific properties of the dielectric that could affect the relationship between $T_{\rm peak}$ and B–O passivation efficacy include 1) high-temperature stability of the film, 2) rate of hydrogen effusion from the film, and 3) concentration of bound hydrogen in the film that is available to be released in

the right form into the silicon (which may or may not correlate directly with the hydrogen bond density in the film).

V. Conclusion

In this paper, the presence of a hydrogen source and a suitable thermal anneal with the hydrogen source present have both been shown to be necessary for B O passivation. The presented results support a hydrogen-based model for B–O passivation while clarifying the role of plasma as supporting the diffusion of the passivating species. It was also shown that permanent passivation of B–O defects is 1) not a purely thermal process and 2) can be enabled by short anneals at temperatures as low as ∼500 °C. For the samples processed in this study, the optimum peak firing temperature for achieving good surface and bulk passivation was found to be 670 °C, with B–O passivation efficacy and $J_{0\mathrm{E}}$ found to decrease with increasing temperature. These observations suggest that hydrogen plays a critical role in B–O passivation and supports a hydrogen-based mechanism wherein net retention of hydrogen within the wafer determines the level of B–O passivation achieved. While other mechanisms, such as B–O passivation through the action of BNPs, cannot be ruled out, they may need to be revised in order to account for the role of hydrogen and for the occurrence of permanent B–O passivation in wafers fired at temperatures as low as ∼500 °C.

Acknowledgment

The authors would like to acknowledge Roth & Rau and Meyer Burger for the MAiA PECVD system used in this study, as well as N. Borojevic, L. Mai, A. Li, and S. Winderbaum for help with sample processing.

References

[1] A. Herguth, G. Schubert, M. Kaes, and G. Hahn, "A new approach to prevent the negative impact of the metastable defect in boron doped Cz silicon solar cells," in *Proc. 4th IEEE World Conf. Photovoltaic Energy Convers.* 2006, vol. 1, pp. 940–943.

[2] A. Herguth, G. Schubert, M. Kaes, and G. Hahn, "Investigations on the long time behavior of the metastable boron–oxygen complex in crystalline silicon," *Prog. Photovoltaics: Res. Appl.*, vol. 16, pp. 135–140, 2008.

[3] A. Herguth and G. Hahn, "Kinetics of the boron-oxygen related defect in theory and experiment," *J. Appl. Phys.*, vol. 108, p. 114509, 2010.

[4] K. A. Münzer, "Hydrogenated silicon nitride for regeneration of light induced degradation," in *Proc. 24th Eur. Photovoltaic Sol. Energy Conf. Exhib.*, 2009, pp. 1558–1561.

[5] G. Krugel, W. Wolke, J. Geilker, S. Rein, and R. Preu, "Impact of hydrogen concentration on the regeneration of light induced degradation," *Energy Procedia*, vol. 8, pp. 47–51, 2011.

[6] S. Wilking, S. Ebert, A. Herguth, and G. Hahn, "Influence of hydrogen effusion from hydrogenated silicon nitride layers on the regeneration of boron-oxygen related defects in crystalline silicon," *J. Appl. Phys.*, vol. 114, p. 194512, 2013.

[7] D. C. Walter *et al.*, "Effect of rapid thermal annealing on recombination centres in boron-doped Czochralski-grown silicon," *Appl. Phys. Lett.*, vol. 104, p. 042111, 2014.

[8] B. J. Hallam, M. D. Abbott, N. Nampalli, P. G. Hamer, and S. R. Wenham, "Implications of accelerated recombination-active defect complex formation for mitigating light-induced degradation in Czochralski silicon," *IEEE J. Photovoltaics*, 2015, to be published.

[9] S. Wilking, C. Beckh, S. Ebert, A. Herguth, and G. Hahn, "Influence of bound hydrogen states on BO regeneration kinetics and consequences for high-speed regeneration processes," *Sol. Energy Mater. Sol. Cells*, vol. 131, pp. 2–8, 2014.

[10] B. Lim, K. Bothe, and J. Schmidt, "Accelerated deactivation of the boron–oxygen-related recombination centre in crystalline silicon," *Semicond. Sci. Tech.*, vol. 26, p. 095009, 2011.

[11] S. Wilking, A. Herguth, and G. Hahn, "Influence of hydrogen on the regeneration of boron-oxygen related defects in crystalline silicon," *J. Appl. Phys.*, vol. 113, p. 194503, 2013.

[12] B. J. Hallam *et al.*, "Hydrogen passivation of B-O defects in Czochralski silicon," *Energy Procedia*, vol. 38, pp. 561–570, 2013.

[13] V. V. Voronkov, R. Falster, B. Lim, and J. Schmidt, "Permanent recovery of electron lifetime in pre-annealed silicon samples: A model based on Ostwald ripening," *J. Appl. Phys.*, vol. 112, p. 113717, 2012.

[14] V. V. Voronkov and R. Falster, "Light-induced boron-oxygen recombination centres in silicon: understanding their formation and elimination," *Solid State Phenomena*, vols. 205/206, pp. 3–14, 2014.

[15] N. Nampalli, B. Hallam, C. Chan, M. Abbott, and S. R. Wenham, "Evidence for the role of hydrogen in the stabilization of minority carrier lifetime in boron-doped Czochralski silicon," *Appl. Phys. Lett.*, vol. 106, no. 17, p. 173501, 2015.

[16] B. J. Hallam *et al.*, "Advanced hydrogenation of dislocation clusters and boron-oxygen defects in silicon solar cells," *Energy Procedia*, 2015, to be published.

[17] N. Nampalli, B. Hallam, C. Chan, M. Abbott, and S. R. Wenham, "Role of hydrogen in the permanent passivation of boron-oxygen defects in Czochralski silicon," in *Proc. 42nd IEEE Photovoltaic Spec. Conf.*, 2015.

[18] R. A. Sinton and A. Cuevas, "Contactless determination of current-voltage characteristics and minority-carrier lifetimes in semiconductors from quasi-steady-state photoconductance data," *Appl. Phys. Lett.*, vol. 69, pp. 2150–2512, 1996.

[19] B. Sopori, "Silicon solar-cell processing for minimizing the influence of impurities and defects," *J. Electron. Mater.*, vol. 31, no. 10, pp. 972–980, 2002.

[20] R. Bousbih, W. Dimassi, I. Haddadi, and H. Ezzaouia, "The effect of thermal annealing on the properties of PECVD hydrogenated silicon nitride," *Phys. Status Solidi C*, vol. 9, nos. 10/11, pp. 2189–2193, 2012.

Authors' photographs and biographies not available at the time of publication.